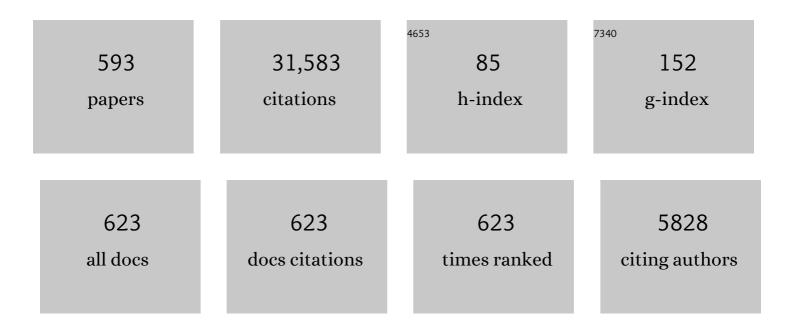
List of Publications by Year in descending order

Source: https://exaly.com/author-pdf/608231/publications.pdf Version: 2024-02-01



#	Article	IF	CITATIONS
1	The THEMIS Fluxgate Magnetometer. Space Science Reviews, 2008, 141, 235-264.	3.7	1,050
2	Bursty bulk flows in the inner central plasma sheet. Journal of Geophysical Research, 1992, 97, 4027-4039.	3.3	980
3	The Magnetospheric Multiscale Magnetometers. Space Science Reviews, 2016, 199, 189-256.	3.7	896
4	Neutral line model of substorms: Past results and present view. Journal of Geophysical Research, 1996, 101, 12975-13010.	3.3	861
5	Characteristics of highâ€speed ion flows in the plasma sheet. Journal of Geophysical Research, 1990, 95, 3801-3809.	3.3	650
6	Statistical characteristics of bursty bulk flow events. Journal of Geophysical Research, 1994, 99, 21257.	3.3	642
7	Average plasma properties in the central plasma sheet. Journal of Geophysical Research, 1989, 94, 6597-6606.	3.3	595
8	Electron-scale measurements of magnetic reconnection in space. Science, 2016, 352, aaf2939.	6.0	545
9	The terrestrial ring current: Origin, formation, and decay. Reviews of Geophysics, 1999, 37, 407-438.	9.0	523
10	Braking of high-speed flows in the near-Earth tail. Geophysical Research Letters, 1997, 24, 1179-1182.	1.5	422
11	The FIELDS Instrument Suite on MMS: Scientific Objectives, Measurements, and Data Products. Space Science Reviews, 2016, 199, 105-135.	3.7	390
12	The magnetopause for large magnetic shear: AMPTE/IRM observations. Journal of Geophysical Research, 1986, 91, 11099-11115.	3.3	384
13	Motion of the dipolarization front during a flow burst event observed by Cluster. Geophysical Research Letters, 2002, 29, 3-1-3-4.	1.5	355
14	Advanced Space Plasma Physics. , 1997, , .		333
15	The magnetosheath region adjacent to the dayside magnetopause: AMPTE/IRM observations. Journal of Geophysical Research, 1994, 99, 121.	3.3	329
16	Basic Space Plasma Physics. , 1996, , .		324
17	Current understanding of magnetic storms: Storm-substorm relationships. Journal of Geophysical Research, 1998, 103, 17705-17728.	3.3	309
18	Spatial scale of high-speed flows in the plasma sheet observed by Cluster. Geophysical Research Letters, 2004, 31, n/a-n/a.	1.5	291

#	Article	IF	CITATIONS
19	High-speed ion flow, substorm current wedge, and multiple Pi 2 pulsations. Journal of Geophysical Research, 1998, 103, 4491-4507.	3.3	260
20	Earthward flow bursts, auroral streamers, and small expansions. Journal of Geophysical Research, 2001, 106, 10791-10802.	3.3	257
21	The magnetospheric response to 8â€minute period strongâ€amplitude upstream pressure variations. Journal of Geophysical Research, 1989, 94, 2505-2519.	3.3	244
22	Current sheet structure near magnetic X-line observed by Cluster. Geophysical Research Letters, 2003, 30, .	1.5	240
23	Magnetic field investigation of the Venus plasma environment: Expected new results from Venus Express. Planetary and Space Science, 2006, 54, 1336-1343.	0.9	235
24	Joint two-dimensional observations of ground magnetic and ionospheric electric fields associated with auroral zone currents: Current systems associated with local auroral break-ups. Planetary and Space Science, 1981, 29, 431-447.	0.9	221
25	Electron-scale dynamics of the diffusion region during symmetric magnetic reconnection in space. Science, 2018, 362, 1391-1395.	6.0	221
26	Local structure of the magnetotail current sheet: 2001 Cluster observations. Annales Geophysicae, 2006, 24, 247-262.	0.6	220
27	Flow braking and the substorm current wedge. Journal of Geophysical Research, 1999, 104, 19895-19903.	3.3	218
28	The Analyser of Space Plasmas and Energetic Atoms (ASPERA-4) for the Venus Express mission. Planetary and Space Science, 2007, 55, 1772-1792.	0.9	214
29	Substorm dipolarization and recovery. Journal of Geophysical Research, 1999, 104, 24995-25000.	3.3	213
30	Extended magnetic reconnection at the Earth's magnetopause from detection of bi-directional jets. Nature, 2000, 404, 848-850.	13.7	212
31	Current sheet flapping motion and structure observed by Cluster. Geophysical Research Letters, 2003, 30, .	1.5	196
32	Multipoint analysis of a bursty bulk flow event on April 11, 1985. Journal of Geophysical Research, 1996, 101, 4967-4989.	3.3	184
33	Substorm Current Wedge Revisited. Space Science Reviews, 2015, 190, 1-46.	3.7	184
34	Upstream pressure variations associated with the bow shock and their effects on the magnetosphere. Journal of Geophysical Research, 1990, 95, 3773-3786.	3.3	179
35	Characteristics of ion flow in the quiet state of the inner plasma sheet. Geophysical Research Letters, 1993, 20, 1711-1714.	1.5	177
36	Electric current and magnetic field geometry in flapping magnetotail current sheets. Annales Geophysicae, 2005, 23, 1391-1403.	0.6	171

#	Article	IF	CITATIONS
37	CHEOPS: A transit photometry mission for ESA's small mission programme. EPJ Web of Conferences, 2013, 47, 03005.	0.1	169
38	The loss of ions from Venus through the plasma wake. Nature, 2007, 450, 650-653.	13.7	168
39	Threeâ€dimensional current flow and particle precipitation in a westward travelling surge (observed) Tj ETQq1 1	0.784314 3.3	rgBT/Overlo 160
40	The transient response mechanism and Pi2 pulsations at substorm onset—Review and outlook. Planetary and Space Science, 1984, 32, 1361-1370.	0.9	157
41	Average ion moments in the plasma sheet boundary layer. Journal of Geophysical Research, 1988, 93, 11507-11520.	3.3	154
42	Multiple overshoot and rebound of a bursty bulk flow. Geophysical Research Letters, 2010, 37, .	1.5	153
43	Cluster observation of a bifurcated current sheet. Geophysical Research Letters, 2003, 30, .	1.5	142
44	Studies of polar current systems using the IMS Scandinavian magnetometer array. Space Science Reviews, 1993, 63, 245-390.	3.7	140
45	The near-Earth plasma sheet: An AMPTE/IRM perspective. Space Science Reviews, 1993, 64, 141-163.	3.7	140
46	The CHEOPS mission. Experimental Astronomy, 2021, 51, 109-151.	1.6	140
47	Ionospheric and field-aligned current systems in the auroral zone: a concise review. Advances in Space Research, 1982, 2, 55-62.	1.2	138
48	Structure of the dayside magnetopause for low magnetic shear. Journal of Geophysical Research, 1993, 98, 13409-13422.	3.3	138
49	The Solar Orbiter magnetometer. Astronomy and Astrophysics, 2020, 642, A9.	2.1	136
50	Ionospheric and Birkeland current distributions for northward interplanetary magnetic field: Inferred polar convection. Journal of Geophysical Research, 1984, 89, 7453-7458.	3.3	135
51	Solar wind dynamic pressure variations and transient magnetospheric signatures. Geophysical Research Letters, 1989, 16, 13-16.	1.5	133
52	The Plasma Instrument for AMPTE IRM. IEEE Transactions on Geoscience and Remote Sensing, 1985, GE-23, 262-266.	2.7	132
53	Energetic electron acceleration in the downstream reconnection outflow region. Journal of Geophysical Research, 2007, 112, n/a-n/a.	3.3	131
54	The Double Star magnetic field investigation: instrument design, performance and highlights of the first year's observations. Annales Geophysicae, 2005, 23, 2713-2732.	0.6	129

#	Article	IF	CITATIONS
55	Evolution of dipolarization in the near-Earth current sheet induced by Earthward rapid flux transport. Annales Geophysicae, 2009, 27, 1743-1754.	0.6	129
56	Flow bursts and auroral activations: Onset timing and foot point location. Journal of Geophysical Research, 2001, 106, 10777-10789.	3.3	128
5 <b>7</b>	Orientation and propagation of current sheet oscillations. Geophysical Research Letters, 2004, 31, n/a-n/a.	1.5	128
58	A statistical and event study of magnetotail dipolarization fronts. Annales Geophysicae, 2011, 29, 1537-1547.	0.6	128
59	First Results of the THEMIS Search Coil Magnetometers. Space Science Reviews, 2008, 141, 509-534.	3.7	122
60	Low-frequency waves in the near-Earth plasma sheet. Journal of Geophysical Research, 1995, 100, 9605.	3.3	121
61	Rapid flux transport in the central plasma sheet. Journal of Geophysical Research, 2001, 106, 301-313.	3.3	115
62	Fast flow during current sheet thinning. Geophysical Research Letters, 2002, 29, 55-1-55-4.	1.5	114
63	Survey of large-amplitude flapping motions in the midtail current sheet. Annales Geophysicae, 2006, 24, 2015-2024.	0.6	112
64	Dynamics of thin current sheets associated with magnetotail reconnection. Journal of Geophysical Research, 2006, 111, .	3.3	109
65	Cluster observations of energetic electrons and electromagnetic fields within a reconnecting thin current sheet in the Earth's magnetotail. Journal of Geophysical Research, 2008, 113, .	3.3	109
66	Magnetic Reconnection in the Near Venusian Magnetotail. Science, 2012, 336, 567-570.	6.0	109
67	A wavy twisted neutral sheet observed by CLUSTER. Geophysical Research Letters, 2002, 29, 5-1-5-4.	1.5	107
68	Loss of hydrogen and oxygen from the upper atmosphere of Venus. Planetary and Space Science, 2006, 54, 1445-1456.	0.9	106
69	Magnetospheric Multiscale observations of magnetic reconnection associated with Kelvinâ€Helmholtz waves. Geophysical Research Letters, 2016, 43, 5606-5615.	1.5	104
70	Pressure changes in the plasma sheet during substorm injections. Journal of Geophysical Research, 1992, 97, 2973-2983.	3.3	102
71	Mars Express and Venus Express multi-point observations of geoeffective solar flare events in December 2006. Planetary and Space Science, 2008, 56, 873-880.	0.9	102
72	Solar wind control of the radial distance of the magnetic reconnection site in the magnetotail. Journal of Geophysical Research, 2005, 110, .	3.3	101

#	Article	IF	CITATIONS
73	Dynamics of the AMPTE artificial comet. Nature, 1986, 320, 720-723.	13.7	99
74	Characteristics of eastward drifting omega bands in the morning sector of the auroral oval. Journal of Geophysical Research, 1983, 88, 9171-9185.	3.3	98
75	Six transiting planets and a chain of Laplace resonances in TOI-178. Astronomy and Astrophysics, 2021, 649, A26.	2.1	94
76	Can flow bursts penetrate into the inner magnetosphere?. Geophysical Research Letters, 2011, 38, n/a-n/a.	1.5	93
77	Magnetosphere-Ionosphere Coupling. , 1993, , .		92
78	Electron scale structures and magnetic reconnection signatures in the turbulent magnetosheath. Geophysical Research Letters, 2016, 43, 5969-5978.	1.5	92
79	Global distribution of ionospheric and fieldâ€aligned currents during substorms as determined from six IMS meridian chains of magnetometers: Initial results. Journal of Geophysical Research, 1982, 87, 8228-8240.	3.3	91
80	Hemispherical Joule heating and the <i>AE</i> indices. Journal of Geophysical Research, 1984, 89, 383-388.	3.3	90
81	A comparison of ULF fluctuations in the solar wind, magnetosheath, and dayside magnetosphere: 1. Magnetosheath morphology. Journal of Geophysical Research, 1991, 96, 3441-3454.	3.3	90
82	The Electron Drift Instrument on Cluster: overview of first results. Annales Geophysicae, 2001, 19, 1273-1288.	0.6	89
83	Superposed epoch analysis of the substorm plasma sheet. Journal of Geophysical Research, 1991, 96, 11605-11608.	3.3	88
84	Ion distributions and flows near the neutral sheet. Journal of Geophysical Research, 1991, 96, 5631-5649.	3.3	88
85	Multi-spacecraft observation of plasma dipolarization/injection in the inner magnetosphere. Annales Geophysicae, 2007, 25, 801-814.	0.6	88
86	Observations of Double Layers in Earth's Plasma Sheet. Physical Review Letters, 2009, 102, 155002.	2.9	88
87	Modes of convection in the magnetotail. Physics of Plasmas, 2002, 9, 3665-3667.	0.7	87
88	How typical are atypical current sheets?. Geophysical Research Letters, 2005, 32, .	1.5	86
89	New Features of Electron Phase Space Holes Observed by the THEMIS Mission. Physical Review Letters, 2009, 102, 225004.	2.9	86
90	Geotail encounter with reconnection diffusion region in the Earth's magnetotail: Evidence of multiple X lines collisionless reconnection?. Journal of Geophysical Research, 2004, 109, .	3.3	85

#	Article	IF	CITATIONS
91	Determination of the polytropic index in the plasma sheet. Geophysical Research Letters, 1989, 16, 295-298.	1.5	84
92	Magnetic turbulence in the plasma sheet. Journal of Geophysical Research, 2004, 109, .	3.3	83
93	Thin Current Sheets in the Magnetotail Observed by Cluster. Space Science Reviews, 2006, 122, 29-38.	3.7	83
94	Dynamics of thin current sheets: Cluster observations. Annales Geophysicae, 2007, 25, 1365-1389.	0.6	83
95	Characteristic size and shape of the mirror mode structures in the solar wind at 0.72 AU. Geophysical Research Letters, 2008, 35, .	1.5	83
96	AMPTE IRM observations of waves associated with flux transfer events in the magnetosphere. Journal of Geophysical Research, 1987, 92, 5827-5843.	3.3	82
97	Waveform and packet structure of lion roars. Annales Geophysicae, 1999, 17, 1528-1534.	0.6	82
98	Cluster observations of an ionâ€scale current sheet in the magnetotail under the presence of a guide field. Journal of Geophysical Research, 2008, 113, .	3.3	80
99	Simultaneous observation of Pc 3–4 pulsations in the solar wind and in the Earth's magnetosphere. Journal of Geophysical Research, 1987, 92, 10053-10062.	3.3	79
100	Little or no solar wind enters Venus' atmosphere at solar minimum. Nature, 2007, 450, 654-656.	13.7	79
101	Electron flatâ€ŧop distributions around the magnetic reconnection region. Journal of Geophysical Research, 2008, 113, .	3.3	78
102	Basic Space Plasma Physics. , 2012, , .		78
103	BepiColombo - Mission Overview and Science Goals. Space Science Reviews, 2021, 217, 1.	3.7	76
104	Magnetotail reconnection onset caused by electron kinetics with a strong external driver. Nature Communications, 2020, 11, 5049.	5.8	75
105	Reconstruction of the magnetotail current sheet structure using multi-point Cluster measurements. Planetary and Space Science, 2005, 53, 237-243.	0.9	74
106	The magnetopause and boundary layer for small magnetic shear: Convection electric fields and reconnection. Geophysical Research Letters, 1990, 17, 1829-1832.	1.5	73
107	MMS Observation of Magnetic Reconnection in the Turbulent Magnetosheath. Journal of Geophysical Research: Space Physics, 2017, 122, 11,442.	0.8	73
108	THE ELECTRON DRIFT INSTRUMENT FOR CLUSTER. Space Science Reviews, 1997, 79, 233-269.	3.7	72

#	Article	IF	CITATIONS
109	Resonant Alfvén waves excited by a sudden impulse. Journal of Geophysical Research, 1984, 89, 2765-2769.	3.3	71
110	Pressure balance between lobe and plasma sheet. Geophysical Research Letters, 1990, 17, 45-48.	1.5	71
111	Ion loss on Mars caused by the Kelvin–Helmholtz instability. Planetary and Space Science, 2004, 52, 1157-1167.	0.9	71
112	Oscillatory magnetic flux tube slippage in the plasma sheet. Annales Geophysicae, 2006, 24, 1695-1704.	0.6	71
113	Initial Venus Express magnetic field observations of the Venus bow shock location at solar minimum. Planetary and Space Science, 2008, 56, 785-789.	0.9	71
114	Investigating Mercury's Environment with the Two-Spacecraft BepiColombo Mission. Space Science Reviews, 2020, 216, 1.	3.7	71
115	Magnetotail energy storage and release during the CDAW 6 substorm analysis intervals. Journal of Geophysical Research, 1985, 90, 1205-1216.	3.3	70
116	Thinning and stretching of the plasma sheet. Journal of Geophysical Research, 2007, 112, .	3.3	70
117	The fluxgate magnetometer of the BepiColombo Mercury Planetary Orbiter. Planetary and Space Science, 2010, 58, 287-299.	0.9	70
118	Event study on pre-substorm phases and their relation to the energy coupling between solar wind and magnetosphere. Planetary and Space Science, 1982, 30, 371-388.	0.9	68
119	Magnetospheric convection observed between 0600 and 2100 LT: Variations with <i>Kp</i> . Journal of Geophysical Research, 1985, 90, 393-398.	3.3	67
120	Estimation of electric fields and currents from international magnetospheric study magnetometer data for the CDAW 6 intervals: Implications for substorm dynamics. Journal of Geophysical Research, 1985, 90, 1305-1317.	3.3	65
121	On the thermodynamics of the plasma sheet. Journal of Geophysical Research, 1991, 96, 20991-20998.	3.3	64
122	Location of the bow shock and ion composition boundaries at Venus—initial determinations from Venus Express ASPERA-4. Planetary and Space Science, 2008, 56, 780-784.	0.9	64
123	Electron acceleration signatures in the magnetotail associated with substorms. Journal of Geophysical Research, 2010, 115, .	3.3	64
124	Electron-Scale Quadrants of the Hall Magnetic Field Observed by the Magnetospheric Multiscale spacecraft during Asymmetric Reconnection. Physical Review Letters, 2017, 118, 175101.	2.9	64
125	Magnetic field fluctuations across the Earth's bow shock. Annales Geophysicae, 2001, 19, 275-287.	0.6	63
126	Collisionless magnetic reconnection in space plasmas. Frontiers in Physics, 2013, 1, .	1.0	63

#	Article	IF	CITATIONS
127	The duskside plasmapause/ring current interface: Convection and plasma wave observations. Journal of Geophysical Research, 1988, 93, 2573-2590.	3.3	62
128	Mirror mode structures observed in the dawn-side magnetosheath by Equator-S. Geophysical Research Letters, 1999, 26, 2159-2162.	1.5	62
129	Multi-scale magnetic field intermittence in the plasma sheet. Annales Geophysicae, 2003, 21, 1955-1964.	0.6	62
130	Observations of kinetic ballooning/interchange instability signatures in the magnetotail. Geophysical Research Letters, 2012, 39, .	1.5	62
131	A flux transfer event observed at the magnetopause by the Equator-S spacecraft and in the ionosphere by the CUTLASS HF radar. Annales Geophysicae, 1999, 17, 707-711.	0.6	61
132	Initial Venus Express magnetic field observations of the magnetic barrier at solar minimum. Planetary and Space Science, 2008, 56, 790-795.	0.9	61
133	Hemispheric asymmetry of the magnetic field wrapping pattern in the Venusian magnetotail. Geophysical Research Letters, 2010, 37, .	1.5	61
134	The hot dayside and asymmetric transit of WASP-189 b seen by CHEOPS. Astronomy and Astrophysics, 2020, 643, A94.	2.1	61
135	Plasma sheet thickness during a bursty bulk flow reversal. Journal of Geophysical Research, 2010, 115, .	3.3	60
136	Study of nearâ€Earth reconnection events with Cluster and Double Star. Journal of Geophysical Research, 2008, 113, .	3.3	59
137	Joint twoâ€dimensional observations of ground magnetic and ionospheric electric fields associated with auroral zone currents 1. Threeâ€dimensional current flows associated with a substormâ€intensified eastward electrojet. Journal of Geophysical Research, 1980, 85, 1963-1978.	3.3	58
138	A comparison of ULF fluctuations in the solar wind, magnetosheath, and dayside magnetosphere: 2. Field and plasma conditions in the magnetosheath. Journal of Geophysical Research, 1991, 96, 3455-3464.	3.3	58
139	Plasma and magnetic field behavior across the magnetosheath near local noon. Journal of Geophysical Research, 1995, 100, 9575.	3.3	58
140	A survey of magnetopause FTEs and associated flow bursts in the polar ionosphere. Annales Geophysicae, 2000, 18, 416-435.	0.6	58
141	Double Star/Cluster observation of neutral sheet oscillations on 5 August 2004. Annales Geophysicae, 2005, 23, 2909-2914.	0.6	58
142	Time-dependent magnetospheric configuration and breakup mapping during a substorm. Journal of Geophysical Research, 2011, 116, .	3.3	56
143	Statistical analysis of short large-amplitude magnetic field structures in the vicinity of the quasi-parallel bow shock. Journal of Geophysical Research, 1994, 99, 13315.	3.3	54
144	Experimental determination of the dispersion of waves observed upstream of a quasi-perpendicular shock. Geophysical Research Letters, 1997, 24, 787-790.	1.5	54

#	Article	IF	CITATIONS
145	Azimuthal pressure gradient as driving force of substorm currents. Geophysical Research Letters, 1998, 25, 959-962.	1.5	54
146	Magnetic effects of the substorm current wedge in a "spread-out wire―model and their comparison with ground, geosynchronous, and tail lobe data. Journal of Geophysical Research, 2011, 116, n/a-n/a.	3.3	54
147	Substorms, Storms, and the Near-Earth Tail Journal of Geomagnetism and Geoelectricity, 1996, 48, 177-185.	0.8	54
148	Ionospheric Joule dissipation as a damping mechanism for high latitude ULF pulsations: Observational evidence. Planetary and Space Science, 1984, 32, 1463-1466.	0.9	53
149	Correlations between PiB type magnetic micropulsations, auroras and equivalent current structures during two isolated substorms. Journal of Atmospheric and Solar-Terrestrial Physics, 1981, 43, 933-945.	0.9	52
150	The Electron Drift Instrument for MMS. Space Science Reviews, 2016, 199, 283-305.	3.7	52
151	Orientation, motion, and other properties of flux transfer event structures on September 4, 1984. Journal of Geophysical Research, 1989, 94, 8852-8866.	3.3	51
152	Rapid flux transport and plasma sheet reconfiguration. Journal of Geophysical Research, 2001, 106, 8381-8390.	3.3	51
153	ARRIVAL TIME CALCULATION FOR INTERPLANETARY CORONAL MASS EJECTIONS WITH CIRCULAR FRONTS AND APPLICATION TO <i>STEREO</i> OBSERVATIONS OF THE 2009 FEBRUARY 13 ERUPTION. Astrophysical Journal, 2011, 741, 34.	1.6	51
154	Transit detection of the long-period volatile-rich super-Earth ν2 Lupi d with CHEOPS. Nature Astronomy, 2021, 5, 775-787.	4.2	51
155	Magnetospheric convection observed between 0600 and 2100 LT: Solar wind and IMF dependence. Journal of Geophysical Research, 1985, 90, 6370-6378.	3.3	50
156	Identification of magnetosheath mirror modes in Equator-S magnetic field data. Annales Geophysicae, 1999, 17, 1560-1573.	0.6	50
157	Do BBFs contribute to inner magnetosphere dipolarizations: Concurrent Cluster and Double Star observations. Geophysical Research Letters, 2006, 33, .	1.5	50
158	Equator‣ observations of drift mirror mode waves in the dawnside magnetosphere. Journal of Geophysical Research, 2007, 112, .	3.3	50
159	First identification of mirror mode waves in Venus' magnetosheath?. Geophysical Research Letters, 2008, 35, .	1.5	50
160	Proton/electron temperature ratio in the magnetotail. Annales Geophysicae, 2011, 29, 2253-2257.	0.6	50
161	Transient electron precipitation during oscillatory BBF braking: THEMIS observations and theoretical estimates. Journal of Geophysical Research: Space Physics, 2013, 118, 3065-3076.	0.8	50
162	Ionospheric and Birkeland current distributions inferred from the MAGSAT magnetometer data. Journal of Geophysical Research, 1983, 88, 4875-4884.	3.3	49

#	Article	IF	CITATIONS
163	Superposed epoch analysis of pressure and magnetic field configuration changes in the plasma sheet. Journal of Geophysical Research, 1993, 98, 9249-9258.	3.3	49
164	Two distinct substorm onsets. Journal of Geophysical Research, 2001, 106, 13105-13118.	3.3	49
165	ON ELECTRON-SCALE WHISTLER TURBULENCE IN THE SOLAR WIND. Astrophysical Journal Letters, 2016, 827, L8.	3.0	49
166	Multispacecraft analysis of dipolarization fronts and associated whistler wave emissions using MMS data. Geophysical Research Letters, 2016, 43, 7279-7286.	1.5	49
167	An Electronâ€Scale Current Sheet Without Bursty Reconnection Signatures Observed in the Nearâ€Earth Tail. Geophysical Research Letters, 2018, 45, 4542-4549.	1.5	49
168	Hermean Magnetosphere-Solar Wind Interaction. Space Science Reviews, 2007, 132, 529-550.	3.7	48
169	Ionospheric photoelectrons at Venus: Initial observations by ASPERA-4 ELS. Planetary and Space Science, 2008, 56, 802-806.	0.9	48
170	Comparative analysis of Venus and Mars magnetotails. Planetary and Space Science, 2008, 56, 812-817.	0.9	48
171	Observation of double layer in the separatrix region during magnetic reconnection. Geophysical Research Letters, 2014, 41, 4851-4858.	1.5	48
172	Bursty Bulk Flow Driven Turbulence in the Earth's Plasma Sheet. Space Science Reviews, 2006, 122, 301-311.	3.7	47
173	The THEMIS Fluxgate Magnetometer. , 2009, , 235-264.		47
174	Toward adapted timeâ€dependent magnetospheric models: A simple approach based on tuning the standard model. Journal of Geophysical Research, 2009, 114, .	3.3	47
175	CHEOPS observations of the HD 108236 planetary system: a fifth planet, improved ephemerides, and planetary radii. Astronomy and Astrophysics, 2021, 646, A157.	2.1	47
176	Thinning and expansion of the substorm plasma sheet. Journal of Geophysical Research, 1992, 97, 17173-17175.	3.3	46
177	Neutral sheet oscillations at substorm onset. Journal of Geophysical Research, 1995, 100, 23737.	3.3	46
178	Two types of tangential magnetopause current sheets: Cluster observations and theory. Journal of Geophysical Research, 2011, 116, n/a-n/a.	3.3	46
179	The roles of direct input of energy from the solar wind and unloading of stored magnetotail energy in driving magnetospheric substorms. Space Science Reviews, 1988, 46, 93.	3.7	45
180	Dayside longâ€period magnetospheric pulsations: Solar wind dependence. Journal of Geophysical Research, 1988, 93, 877-883.	3.3	45

#	Article	IF	CITATIONS
181	The BepiColombo Planetary Magnetometer MPO-MAG: What Can We Learn from the Hermean Magnetic Field?. Space Science Reviews, 2021, 217, 1.	3.7	45
182	Mirrorâ€modeâ€like structures in Venus' induced magnetosphere. Journal of Geophysical Research, 2008, 113, .	3.3	44
183	Induced magnetosphere and its outer boundary at Venus. Journal of Geophysical Research, 2008, 113, .	3.3	44
184	Current Systems in Planetary Magnetospheres and Ionospheres. Space Science Reviews, 2010, 152, 99-134.	3.7	44
185	A direct examination of the dynamics of dipolarization fronts using MMS. Journal of Geophysical Research: Space Physics, 2017, 122, 4335-4347.	0.8	44
186	Mirror mode structures in the solar wind at 0.72 AU. Journal of Geophysical Research, 2009, 114, .	3.3	43
187	The BepiColombo mission: An outstanding tool for investigating the Hermean environment. Planetary and Space Science, 2010, 58, 40-60.	0.9	43
188	Disappearing induced magnetosphere at Venus: Implications for closeâ€ <del>i</del> n exoplanets. Geophysical Research Letters, 2009, 36, .	1.5	42
189	Small substorms: Solar wind input and magnetotail dynamics. Journal of Geophysical Research, 2000, 105, 21109-21117.	3.3	41
190	Kinetic ballooning/interchange instability in a bent plasma sheet. Journal of Geophysical Research, 2012, 117, .	3.3	41
191	Ion distributions and flows in and near the plasma sheet boundary layer. Journal of Geophysical Research, 1992, 97, 1449-1460.	3.3	40
192	A sigma–delta fluxgate magnetometer for space applications. Measurement Science and Technology, 2003, 14, 1003-1012.	1.4	40
193	The magnetosphere of Mercury and its solar wind environment: Open issues and scientific questions. Advances in Space Research, 2006, 38, 604-609.	1.2	40
194	Observations of an active thin current sheet. Journal of Geophysical Research, 2008, 113, .	3.3	40
195	Asymmetry in the current sheet and secondary magnetic flux ropes during guide field magnetic reconnection. Journal of Geophysical Research, 2012, 117, .	3.3	40
196	In situ multi-spacecraft and remote imaging observations of the first CME detected by Solar Orbiter and BepiColombo. Astronomy and Astrophysics, 2021, 656, A2.	2.1	40
197	Testing electric field models using ring current ion energy spectra from the Equator-S ion composition (ESIC) instrument. Annales Geophysicae, 1999, 17, 1611-1621.	0.6	39
198	Kink mode oscillation of the current sheet. Geophysical Research Letters, 2003, 30, .	1.5	39

#	Article	IF	CITATIONS
199	Cluster observations of <i>â^,B</i> <sub><i>z</i></sub> / <i>â^,x</i> during growth phase magnetotail stretching intervals. Journal of Geophysical Research: Space Physics, 2013, 118, 5720-5730.	0.8	39
200	Electron pitch angle/energy distribution in the magnetotail. Journal of Geophysical Research: Space Physics, 2014, 119, 7214-7227.	0.8	39
201	MMS Examination of FTEs at the Earth's Subsolar Magnetopause. Journal of Geophysical Research: Space Physics, 2018, 123, 1224-1241.	0.8	39
202	Flow bouncing and electron injection observed by Cluster. Journal of Geophysical Research: Space Physics, 2013, 118, 2055-2072.	0.8	38
203	Analysis of Early Science observations with the CHaracterising ExOPlanets Satellite ( <i>CHEOPS</i> ) using <scp>pycheops</scp> . Monthly Notices of the Royal Astronomical Society, 2022, 514, 77-104.	1.6	38
204	Magnetospheric plasma drifts during a sudden impulse. Journal of Geophysical Research, 1983, 88, 9287-9289.	3.3	37
205	A statistical study of compressional waves in the tail current sheet. Journal of Geophysical Research, 2003, 108, .	3.3	37
206	Dynamics and waves near multiple magnetic null points in reconnection diffusion region. Journal of Geophysical Research, 2009, 114, .	3.3	37
207	A comparative study of dipolarization fronts at MMS and Cluster. Geophysical Research Letters, 2016, 43, 6012-6019.	1.5	37
208	The changing face of AU Mic b: stellar spots, spin-orbit commensurability, and transit timing variations as seen by CHEOPS and TESS. Astronomy and Astrophysics, 2021, 654, A159.	2.1	36
209	Flow shear near the boundary of the plasma sheet observed by Cluster and Geotail. Journal of Geophysical Research, 2004, 109, .	3.3	35
210	Tailward and earthward flow onsets observed by Cluster in a thin current sheet. Journal of Geophysical Research, 2009, 114, .	3.3	35
211	Flux transport, dipolarization, and current sheet evolution during a double-onset substorm. Journal of Geophysical Research, 2011, 116, .	3.3	35
212	Wavelet analysis of magnetic turbulence in the Earth's plasma sheet. Physics of Plasmas, 2004, 11, 1333-1338.	0.7	34
213	Intermittent turbulence, noisy fluctuations, and wavy structures in the Venusian magnetosheath and wake. Journal of Geophysical Research, 2008, 113, .	3.3	34
214	MMS Observation of Asymmetric Reconnection Supported by 3â€Ð Electron Pressure Divergence. Journal of Geophysical Research: Space Physics, 2018, 123, 1806-1821.	0.8	34
215	Structure of the Current Sheet in the 11 July 2017 Electron Diffusion Region Event. Journal of Geophysical Research: Space Physics, 2019, 124, 1173-1186.	0.8	34
216	Solar Wind-Magnetosphere Coupling: Processes and Observations. Physica Scripta, 1987, T18, 61-72.	1.2	33

#	Article	IF	CITATIONS
217	The magnetic field experiment onboard Equator-S and its scientific possibilities. Annales Geophysicae, 1999, 17, 1521-1527.	0.6	33
218	Transition from substorm growth to substorm expansion phase as observed with a radial configuration of ISTP and Cluster spacecraft. Annales Geophysicae, 2005, 23, 2183-2198.	0.6	33
219	Flow burst-induced Kelvin-Helmholtz waves in the terrestrial magnetotail. Geophysical Research Letters, 2007, 34, .	1.5	33
220	Mirror mode structures near Venus and Comet P/Halley. Annales Geophysicae, 2014, 32, 651-657.	0.6	33
221	Spontaneous magnetic reconnection. Astronomy and Astrophysics Review, 2015, 23, 1.	9.1	33
222	Merits and Limitations of the Use of Geomagnetic Indices in Solar Wind-Magnetosphere Coupling Studies. Astrophysics and Space Science Library, 1986, , 3-15.	1.0	33
223	A new method for generating instantaneous ionospheric conductivity models using ground-based magnetic data. Planetary and Space Science, 1986, 34, 713-722.	0.9	32
224	Observation of repeated intense near-Earth reconnection on closed field lines with Cluster, Double Star, and other spacecraft. Geophysical Research Letters, 2007, 34, .	1.5	32
225	A model of electromagnetic electron phase-space holes and its application. Journal of Geophysical Research, 2011, 116, n/a-n/a.	3.3	32
226	Multiscale Currents Observed by MMS in the Flow Braking Region. Journal of Geophysical Research: Space Physics, 2018, 123, 1260-1278.	0.8	32
227	Are earthward bursty bulk flows convective or field-aligned?. Journal of Geophysical Research, 2001, 106, 21211-21215.	3.3	31
228	Response of the inner magnetosphere and the plasma sheet to a sudden impulse. Journal of Geophysical Research, 2008, 113, .	3.3	31
229	Behavior of current sheets at directional magnetic discontinuities in the solar wind at 0.72 AU. Geophysical Research Letters, 2008, 35, .	1.5	31
230	Interaction of Magnetic Flux Ropes Via Magnetic Reconnection Observed at the Magnetopause. Journal of Geophysical Research: Space Physics, 2017, 122, 10,436.	0.8	31
231	Plasma observations on AMPTE/IRM during the lithium releases in the solar wind. Journal of Geophysical Research, 1986, 91, 1271-1281.	3.3	30
232	Plasma and field observations of a compressional Pc 5 wave event. Journal of Geophysical Research, 1987, 92, 12203-12212.	3.3	30
233	Average electric wave spectra across the plasma sheet and their relation to ion bulk speed. Journal of Geophysical Research, 1989, 94, 15221-15230.	3.3	30
234	Observations of electrostatic solitary waves associated with reconnection by Geotail and Cluster. Advances in Space Research, 2006, 37, 1373-1381.	1.2	30

#	Article	IF	CITATIONS
235	TC-1 observations of flux pileup and dipolarization-associated expansion in the near-Earth magnetotail during substorms. Geophysical Research Letters, 2007, 34, .	1.5	30
236	Spectral scaling in the turbulent Earth's plasma sheet revisited. Nonlinear Processes in Geophysics, 2007, 14, 535-541.	0.6	30
237	Highly integrated front-end electronics for spaceborne fluxgate sensors. Measurement Science and Technology, 2008, 19, 115801.	1.4	30
238	Substorm expansion triggered by a sudden impulse front propagating from the dayside magnetopause. Journal of Geophysical Research, 2009, 114, .	3.3	30
239	Oscillatory flow braking in the magnetotail: THEMIS statistics. Geophysical Research Letters, 2013, 40, 2505-2510.	1.5	30
240	Transient, smallâ€scale fieldâ€aligned currents in the plasma sheet boundary layer during storm time substorms. Geophysical Research Letters, 2016, 43, 4841-4849.	1.5	30
241	Coupled dark state magnetometer for the China Seismo-Electromagnetic Satellite. Measurement Science and Technology, 2018, 29, 095103.	1.4	30
242	CHEOPS precision phase curve of the Super-Earth 55 Cancri e. Astronomy and Astrophysics, 2021, 653, A173.	2.1	30
243	A pair of sub-Neptunes transiting the bright K-dwarf TOI-1064 characterized with <i>CHEOPS</i> . Monthly Notices of the Royal Astronomical Society, 2022, 511, 1043-1071.	1.6	30
244	Reply to "Comment on â€~Solar wind dynamic pressure variations and transient magnetospheric signatures‧― Geophysical Research Letters, 1989, 16, 1200-1202.	1.5	29
245	Mirror waves downstream of the quasi-perpendicular bow shock. Journal of Geophysical Research, 1998, 103, 4747-4753.	3.3	29
246	Statistical survey of magnetic field and ion velocity fluctuations in the near-Earth plasma sheet: Active Magnetospheric Particle Trace Explorers/Ion Release Module (AMPTE/IRM) measurements. Journal of Geophysical Research, 2002, 107, SMP 8-1.	3.3	29
247	Magnetic field investigation of Mercury's magnetosphere and the inner heliosphere by MMO/MGF. Planetary and Space Science, 2010, 58, 279-286.	0.9	29
248	Two states of magnetotail dipolarization fronts: A statistical study. Journal of Geophysical Research: Space Physics, 2015, 120, 1096-1108.	0.8	29
249	Formation of current density profile in tilted current sheets. Annales Geophysicae, 2008, 26, 3669-3676.	0.6	29
250	Comment on "Geotail survey of ion flow in the plasma sheet: Observations between 10 and 50 RE―by W. R. Paterson et al Journal of Geophysical Research, 1999, 104, 17521-17525.	3.3	28
251	Observations of plasma vortices in the vicinity of flow-braking: a case study. Annales Geophysicae, 2009, 27, 3009-3017.	0.6	28
252	Mirror mode structures ahead of dipolarization front near the neutral sheet observed by Cluster. Geophysical Research Letters, 2016, 43, 8853-8858.	1.5	28

#	Article	IF	CITATIONS
253	Mio—First Comprehensive Exploration of Mercury's Space Environment: Mission Overview. Space Science Reviews, 2020, 216, 1.	3.7	28
254	Plasma sheet structure during strongly northward IMF. Journal of Geophysical Research, 2003, 108, .	3.3	27
255	Compressional waves in the Earth's neutral sheet. Annales Geophysicae, 2004, 22, 303-315.	0.6	27
256	Plasma flow channels with ULF waves observed by Cluster and Double Star. Annales Geophysicae, 2005, 23, 2929-2935.	0.6	27
257	Kinetic instabilities in the lunar wake: ARTEMIS observations. Journal of Geophysical Research, 2012, 117, .	3.3	27
258	Force balance at the magnetopause determined with MMS: Application to flux transfer events. Geophysical Research Letters, 2016, 43, 11,941.	1.5	27
259	Largeâ€Scale Survey of the Structure of the Dayside Magnetopause by MMS. Journal of Geophysical Research: Space Physics, 2018, 123, 2018-2033.	0.8	27
260	The UV aurora and ionospheric flows during flux transfer events. Annales Geophysicae, 2001, 19, 179-188.	0.6	27
261	Rocket and ground-based study of an auroral breakup event. Planetary and Space Science, 1983, 31, 207-220.	0.9	26
262	Correlated observations of substorm effects in the nearâ€Earth region and the deep magnetotail. Journal of Geophysical Research, 1985, 90, 4021-4026.	3.3	26
263	A model for the electric fields and currents during a strong Ps 6 pulsation event. Journal of Geophysical Research, 1990, 95, 3733-3743.	3.3	26
264	Electric field measurements in the inner magnetosphere by Cluster EDI. Journal of Geophysical Research, 2003, 108, .	3.3	26
265	Propagation of a sudden impulse through the magnetosphere initiating magnetospheric Pc5 pulsations. Journal of Geophysical Research, 2011, 116, n/a-n/a.	3.3	26
266	Multi-scale structures of turbulent magnetic reconnection. Physics of Plasmas, 2016, 23, .	0.7	26
267	The Properties of Lion Roars and Electron Dynamics in Mirror Mode Waves Observed by the Magnetospheric MultiScale Mission. Journal of Geophysical Research: Space Physics, 2018, 123, 93-103.	0.8	26
268	SERENA: Particle Instrument Suite for Determining the Sun-Mercury Interaction from BepiColombo. Space Science Reviews, 2021, 217, 11.	3.7	26
269	The atmosphere and architecture of WASP-189 b probed by its CHEOPS phase curve. Astronomy and Astrophysics, 2022, 659, A74.	2.1	26
270	Flow burst–induced large-scale plasma sheet oscillation. Journal of Geophysical Research, 2004, 109, .	3.3	25

#	Article	IF	CITATIONS
271	THEMIS observations of duskside compressional Pc5 waves. Journal of Geophysical Research, 2009, 114,	3.3	25
272	Fast tailward flows in the plasma sheet boundary layer during a substorm on 9 March 2008: THEMIS observations. Journal of Geophysical Research, 2011, 116, .	3.3	25
273	The distribution of the ring current: Cluster observations. Annales Geophysicae, 2011, 29, 1655-1662.	0.6	25
274	lonospheric response to oscillatory flow braking in the magnetotail. Journal of Geophysical Research: Space Physics, 2013, 118, 1529-1544.	0.8	25
275	BepiColombo Science Investigations During Cruise and Flybys at the Earth, Venus and Mercury. Space Science Reviews, 2021, 217, 1.	3.7	25
276	Spi-OPS: <i>Spitzer</i> and CHEOPS confirm the near-polar orbit of MASCARA-1 b and reveal a hint of dayside reflection. Astronomy and Astrophysics, 2022, 658, A75.	2.1	25
277	Non-stationarity and low frequency turbulence at a quasiperpendicular shock front. Advances in Space Research, 1997, 20, 729-734.	1.2	24
278	Properties of a bifurcated current sheet observed on 29 August 2001. Annales Geophysicae, 2004, 22, 2535-2540.	0.6	24
279	Venus Express observations of an atypically distant bow shock during the passage of an interplanetary coronal mass ejection. Journal of Geophysical Research, 2008, 113, .	3.3	24
280	Cluster EDI convection measurements across the high-latitude plasma sheet boundary at midnight. Annales Geophysicae, 2001, 19, 1669-1681.	0.6	24
281	Joint two-dimensional observations of ground magnetic and ionospheric electric fields associated with auroral zone currents. 2. Three-dimensional current flow in the morning sector during substorm recovery Journal of Geomagnetism and Geoelectricity, 1981, 33, 297-318.	0.8	24
282	Magnetometer and incoherent scatter observations of an intense Ps 6 pulsation event. Journal of Atmospheric and Solar-Terrestrial Physics, 1988, 50, 357-367.	0.9	23
283	The plasma sheet boundary layer and magnetospheric substorms Journal of Geomagnetism and Geoelectricity, 1988, 40, 157-175.	0.8	23
284	High-beta plasma blobs in the morningside plasma sheet. Annales Geophysicae, 1999, 17, 1592-1601.	0.6	23
285	Investigation of the outer and inner low-latitude boundary layers. Annales Geophysicae, 2001, 19, 1065-1088.	0.6	23
286	Equator-S observations of He+energization by EMIC waves in the dawnside equatorial magnetosphere. Geophysical Research Letters, 2002, 29, 74-1-74-4.	1.5	23
287	Coordinated Study on Solar Wind Turbulence During the Venus-Express, ACE and Ulysses Alignment of August 2007. Earth, Moon and Planets, 2009, 104, 101-104.	0.3	23
288	Electron-cylotron maser radiation from electron holes: upward current region. Annales Geophysicae, 2011, 29, 1885-1904.	0.6	23

#	Article	IF	CITATIONS
289	Correlation of core field polarity of magnetotail flux ropes with the IMF <i>B<sub>y</sub></i> : Reconnection guide field dependency. Journal of Geophysical Research: Space Physics, 2014, 119, 2933-2944.	0.8	23
290	Magnetosheath High‧peed Jets: Internal Structure and Interaction With Ambient Plasma. Journal of Geophysical Research: Space Physics, 2017, 122, 10,157.	0.8	23
291	Estimation of ionospheric electric fields and currents from a regional magnetometer array. Journal of Geophysical Research, 1985, 90, 3525-3530.	3.3	22
292	Energetic electron precipitation during a magnetospheric substorm and its relationship to wave particle interaction. Journal of Geophysical Research, 1986, 91, 5711-5718.	3.3	22
293	Magnetospheric lion roars. Annales Geophysicae, 2000, 18, 406-410.	0.6	22
294	Compressional Pc5 type pulsations in the morningside plasma sheet. Annales Geophysicae, 2001, 19, 311-320.	0.6	22
295	Dissipation scales in the Earth's plasma sheet estimated from Cluster measurements. Nonlinear Processes in Geophysics, 2005, 12, 725-732.	0.6	22
296	The Venusian induced magnetosphere: A case study of plasma and magnetic field measurements on the Venus Express mission. Planetary and Space Science, 2008, 56, 796-801.	0.9	22
297	Magnetospheric quasi-static response to the dynamic magnetosheath: A THEMIS case study. Geophysical Research Letters, 2008, 35, .	1.5	22
298	Test of methods to infer the magnetic reconnection geometry from spacecraft data. Journal of Geophysical Research, 2010, 115, .	3.3	22
299	Comparison of accelerated ion populations observed upstream of the bow shocks at Venus and Mars. Annales Geophysicae, 2011, 29, 511-528.	0.6	22
300	Optimized merging of search coil and fluxgate data for MMS. Geoscientific Instrumentation, Methods and Data Systems, 2016, 5, 521-530.	0.6	22
301	A statistical study on the shape and position of the magnetotail neutral sheet. Annales Geophysicae, 2016, 34, 303-311.	0.6	22
302	Some recent progress in substorm studies Journal of Geomagnetism and Geoelectricity, 1986, 38, 633-651.	0.8	22
303	Detection of the tidal deformation of WASP-103b at 3 <i><math>\hat{I}f</math> </i> with CHEOPS. Astronomy and Astrophysics, 2022, 657, A52.	2.1	22
304	lsotropized Magneticâ€Moment Equation of State for the Central Plasma Sheet. Geophysical Research Letters, 1990, 17, 271-274.	1.5	21
305	Geometry of the nearâ€Earth plasma sheet. Journal of Geophysical Research, 1990, 95, 10707-10710.	3.3	21
306	Constructing the magnetospheric model including pressure measurements. Journal of Geophysical Research, 2002, 107, SMP 4-1.	3.3	21

#	Article	IF	CITATIONS
307	A statistical analysis of Pi2â€band waves in the plasma sheet and their relation to magnetospheric drivers. Journal of Geophysical Research: Space Physics, 2015, 120, 6167-6175.	0.8	21
308	Bi-directional electron distributions associated with near-tail flux transport. Geophysical Research Letters, 2001, 28, 3813-3816.	1.5	20
309	Particle Acceleration in Mercury's Magnetosphere. Space Science Reviews, 2007, 132, 593-609.	3.7	20
310	Magnetic fluctuations and turbulence in the Venus magnetosheath and wake. Geophysical Research Letters, 2008, 35, .	1.5	20
311	Period and damping factor of <i>Pi</i> 2 pulsations during oscillatory flow braking in the magnetotail. Journal of Geophysical Research: Space Physics, 2014, 119, 4512-4520.	0.8	20
312	A Statistical Study on the Properties of Dips Ahead of Dipolarization Fronts Observed by MMS. Journal of Geophysical Research: Space Physics, 2019, 124, 139-150.	0.8	20
313	CHEOPS geometric albedo of the hot Jupiter HD 209458 b. Astronomy and Astrophysics, 2022, 659, L4.	2.1	20
314	Comparison of heightâ€integrated current densities derived from groundâ€based magnetometer and rocketâ€borne observations during the Porcupine F3 and F4 flights. Journal of Geophysical Research, 1983, 88, 8063-8072.	3.3	19
315	Electric fields and currents associated with active aurora. Geophysical Monograph Series, 1984, , 77-85.	0.1	19
316	Multi-scale analysis of turbulence in the Earth's current sheet. Annales Geophysicae, 2004, 22, 2525-2533.	0.6	19
317	Cluster and Double Star observations of dipolarization. Annales Geophysicae, 2005, 23, 2915-2920.	0.6	19
318	First observation of energetic neutral atoms in the Venus environment. Planetary and Space Science, 2008, 56, 807-811.	0.9	19
319	The BepiColombo–Mio Magnetometer en Route to Mercury. Space Science Reviews, 2020, 216, 1.	3.7	19
320	Substorm activity in Venus's magnetotail. Annales Geophysicae, 2009, 27, 2321-2330.	0.6	18
321	Cross-scale: multi-scale coupling in space plasmas. Experimental Astronomy, 2009, 23, 1001-1015.	1.6	18
322	X line distribution determined from earthward and tailward convective bursty flows in the central plasma sheet. Journal of Geophysical Research, 2010, 115, .	3.3	18
323	Evolution of a typical ionâ€scale magnetic flux rope caused by thermal pressure enhancement. Journal of Geophysical Research: Space Physics, 2017, 122, 2040-2050.	0.8	18
324	Exploiting timing capabilities of the CHEOPS mission with warm-Jupiter planets. Monthly Notices of the Royal Astronomical Society, 2021, 506, 3810-3830.	1.6	18

#	Article	IF	CITATIONS
325	A search for transiting planets around hot subdwarfs. Astronomy and Astrophysics, 2021, 650, A205.	2.1	18
326	A model of so-called "Zebra" emissions in solar flare radio burst continua. Annales Geophysicae, 2011, 29, 1673-1682.	0.6	18
327	Total current of the auroral electrojet estimated from the IMS Alaska meridian chain of magnetic observatories. Planetary and Space Science, 1982, 30, 621-625.	0.9	17
328	Multi-point observation of the high-speed flows in the plasma sheet. Advances in Space Research, 2005, 36, 1444-1447.	1.2	17
329	Cluster vision of the magnetotail current sheet on a macroscale. Journal of Geophysical Research, 2005, 110, .	3.3	17
330	Mode conversion between Alfvén and slow waves observed in the magnetotail by THEMIS. Geophysical Research Letters, 2011, 38, n/a-n/a.	1.5	17
331	Jet front-driven mirror modes and shocklets in the near-Earth flow-braking region. Geophysical Research Letters, 2011, 38, n/a-n/a.	1.5	17
332	Evidence of the origin of the Hall magnetic field for reconnection: Hall MHD reconstruction results from Cluster observations. Journal of Geophysical Research, 2011, 116, n/a-n/a.	3.3	17
333	Electron-cylotron maser radiation from electron holes: downward current region. Annales Geophysicae, 2012, 30, 119-130.	0.6	17
334	Interinstrument calibration using magnetic field data from the flux-gate magnetometer (FGM) and electron drift instrument (EDI) onboard Cluster. Geoscientific Instrumentation, Methods and Data Systems, 2014, 3, 1-11.	0.6	17
335	Simultaneous Remote Observations of Intense Reconnection Effects by DMSP and MMS Spacecraft During a Storm Time Substorm. Journal of Geophysical Research: Space Physics, 2017, 122, 10891-10909.	0.8	17
336	Three-dimensional Birkeland-ionospheric current system determined from MAGSAT. Geophysical Monograph Series, 1984, , 123-130.	0.1	16
337	Simultaneous observation of the plasma sheet in the near Earth and distant magnetotail: ISEEâ€1 and ISEEâ€3. Geophysical Research Letters, 1984, 11, 1034-1037.	1.5	16
338	A statistical survey of the magnetotail current sheet. Advances in Space Research, 2006, 38, 1834-1837.	1.2	16
339	Convective bursty flows in the nearâ€Earth magnetotail inside 13 R <sub>E</sub> . Journal of Geophysical Research, 2009, 114, .	3.3	16
340	Statistical study of lowâ€frequency magnetic field fluctuations near Venus under the different interplanetary magnetic field orientations. Journal of Geophysical Research, 2010, 115, .	3.3	16
341	Giant flux ropes observed in the magnetized ionosphere at Venus. Geophysical Research Letters, 2012, 39, .	1.5	16
342	Plasma Density Estimates From Spacecraft Potential Using MMS Observations in the Dayside Magnetosphere. Journal of Geophysical Research: Space Physics, 2018, 123, 2620-2629.	0.8	16

#	Article	IF	CITATIONS
343	Multi-point analysis of coronal mass ejection flux ropes using combined data from Solar Orbiter, BepiColombo, and Wind. Astronomy and Astrophysics, 2021, 656, A13.	2.1	16
344	Spatial structure of plasma flow associated turbulence in the Earth's plasma sheet. Annales Geophysicae, 2007, 25, 13-17.	0.6	16
345	Dynamics of longâ€period ULF waves in the plasma sheet: Coordinated space and ground observations. Journal of Geophysical Research, 2012, 117, .	3.3	15
346	Wave telescope technique for MMS magnetometer. Geophysical Research Letters, 2016, 43, 4774-4780.	1.5	15
347	Near-Earth plasma sheet boundary dynamics during substorm dipolarization. Earth, Planets and Space, 2017, 69, 129.	0.9	15
348	Dissipation of Earthward Propagating Flux Rope Through Reâ€reconnection with Geomagnetic Field: An MMS Case Study. Journal of Geophysical Research: Space Physics, 2019, 124, 7477-7493.	0.8	15
349	On the deviation from Maxwellian of the ion velocity distribution functions in the turbulentÂmagnetosheath. Journal of Plasma Physics, 2020, 86, .	0.7	15
350	The EBLM project – VIII. First results for M-dwarf mass, radius, and effective temperature measurements using <i>CHEOPS</i> light curves. Monthly Notices of the Royal Astronomical Society, 2021, 506, 306-322.	1.6	15
351	The Magnetospheric Multiscale Magnetometers. , 2017, , 189-256.		15
352	Dayside equatorialâ€plane convection and IMF sector structure. Journal of Geophysical Research, 1986, 91, 4557-4560.	3.3	14
353	Propagation of perturbation energy fluxes in the subsolar magnetosheath: AMPTE IRM observations. Geophysical Research Letters, 1991, 18, 1667-1670.	1.5	14
354	High- and low-altitude observations of adiabatic parameters associated with auroral electron acceleration. Journal of Geophysical Research, 2000, 105, 2541-2550.	3.3	14
355	Lion roar trapping in mirror modes. Geophysical Research Letters, 2000, 27, 1843-1846.	1.5	14
356	Evidence for an extended reconnection line at the dayside magnetopause. Earth, Planets and Space, 2001, 53, 619-625.	0.9	14
357	Cross-scale coupling-induced intermittency near interplanetary shocks. Journal of Geophysical Research, 2006, 111, .	3.3	14
358	Magnetotail dipolarization and associated current systems observed by Cluster and Double Star. Journal of Geophysical Research, 2008, 113, .	3.3	14
359	Magnetosheath fluctuations at Venus for two extreme orientations of the interplanetary magnetic field. Geophysical Research Letters, 2009, 36, .	1.5	14
360	First application of a Petschekâ€ŧype reconnection model with timeâ€varying reconnection rate to THEMIS observations. Journal of Geophysical Research, 2009, 114, .	3.3	14

#	Article	IF	CITATIONS
361	Flux-gate magnetometer spin axis offset calibration using the electron drift instrument. Measurement Science and Technology, 2014, 25, 105008.	1.4	14
362	Threeâ€dimensional development of front region of plasma jets generated by magnetic reconnection. Geophysical Research Letters, 2016, 43, 8356-8364.	1.5	14
363	Steepening of waves at the duskside magnetopause. Geophysical Research Letters, 2016, 43, 7373-7380.	1.5	14
364	Magnetotail energy dissipation during an auroralÂsubstorm. Nature Physics, 2016, 12, 1158-1163.	6.5	14
365	Ionospheric Footprints of Detached Magnetotail Interchange Heads. Geophysical Research Letters, 2019, 46, 7237-7247.	1.5	14
366	Particle trapping at a tangential discontinuity: Multiple incidence. Planetary and Space Science, 1988, 36, 1477-1484.	0.9	13
367	A hybrid equation of state for the quasiâ€static central plasma sheet. Geophysical Research Letters, 1992, 19, 421-424.	1.5	13
368	The MHD structure of the plasmasheet boundary: (1) Tangential momentum balance and consistency with slow mode shocks. Geophysical Research Letters, 1992, 19, 2083-2086.	1.5	13
369	A search for upstream pressure pulses associated with flux transfer events: An AMPTE/ISEE case study. Journal of Geophysical Research, 1994, 99, 13521.	3.3	13
370	Observations of a very thin shock. Advances in Space Research, 1999, 24, 47-50.	1.2	13
371	A case study of a radially polarized Pc4 event observed by the Equator-S satellite. Annales Geophysicae, 2000, 18, 411-415.	0.6	13
372	Correlation studies of compressional Pc5 pulsations in space and Ps6 pulsations on the ground. Journal of Geophysical Research, 2001, 106, 29797-29806.	3.3	13
373	Relationship between ULF waves and radiation belt electrons during the March 10, 1998, storm. Advances in Space Research, 2002, 30, 2163-2168.	1.2	13
374	Neutral sheet normal direction determination. Advances in Space Research, 2005, 36, 1940-1945.	1.2	13
375	Deformation and evolution of solar wind discontinuities through their interactions with the Earth's bow shock. Journal of Geophysical Research, 2009, 114, .	3.3	13
376	Magnetic guide field generation in collisionless current sheets. Annales Geophysicae, 2010, 28, 789-793.	0.6	13
377	Deriving plasma densities in tenuous plasma regions, with the spacecraft potential under active control. Journal of Geophysical Research: Space Physics, 2015, 120, 9594-9616.	0.8	13
378	Bursty bulk flows at different magnetospheric activity levels: Dependence on IMF conditions. Journal of Geophysical Research: Space Physics, 2016, 121, 8773-8789.	0.8	13

#	Article	IF	CITATIONS
379	Study of the spacecraft potential under active control and plasma density estimates during the MMS commissioning phase. Geophysical Research Letters, 2016, 43, 4858-4864.	1.5	13
380	BBF Deceleration Downâ€Tail of X < â^'15 R E From MMS Observation. Journal of Geophysical Research: Space Physics, 2020, 125, e2019JA026837.	0.8	13
381	Bi-directional electrons in the near-Earth plasma sheet. Annales Geophysicae, 2003, 21, 1497-1507.	0.6	13
382	Alfvén waves in the near-PSBL lobe: Cluster observations. Annales Geophysicae, 2006, 24, 1001-1013.	0.6	13
383	Experimental method for identification of dispersive three-wave coupling in space plasma. Advances in Space Research, 2000, 25, 1571-1577.	1.2	12
384	Tail lobe convection observed by Cluster/EDI. Journal of Geophysical Research, 2003, 108, .	3.3	12
385	On the venus bow shock compressibility. Advances in Space Research, 2004, 33, 1920-1923.	1.2	12
386	Spacecraft potential control for Double Star. Annales Geophysicae, 2005, 23, 2813-2823.	0.6	12
387	Electron dynamics in the reconnection ion diffusion region. Journal of Geophysical Research, 2012, 117, .	3.3	12
388	Cluster as current sheet surveyor in the magnetotail. Annales Geophysicae, 2013, 31, 1605-1610.	0.6	12
389	X lines in the magnetotail for southward and northward IMF conditions. Journal of Geophysical Research: Space Physics, 2015, 120, 7764-7773.	0.8	12
390	Design of the Magnetoresistive Magnetometer for ESA's SOSMAG Project. IEEE Transactions on Magnetics, 2015, 51, 1-4.	1.2	12
391	Weak, Quiet Magnetic Fields Seen in the Venus Atmosphere. Scientific Reports, 2016, 6, 23537.	1.6	12
392	Transit timing variations of AU Microscopii b and c. Astronomy and Astrophysics, 2022, 659, L7.	2.1	12
393	Average electric wave spectra in the plasma sheet: Dependence on ion density and ion beta. Journal of Geophysical Research, 1990, 95, 3811-3817.	3.3	11
394	Equator-S observation of reconnection coupled to surface waves. Advances in Space Research, 2002, 29, 1129-1134.	1.2	11
395	Equator-S observations of boundary signatures: FTE's or Kelvin-Helmholtz waves?. Geophysical Monograph Series, 2003, , 205-210.	0.1	11
396	Statistical survey of magnetic and velocity fluctuations in the near-Earth plasma sheet: International Sun Earth Explorer (ISEE-2) measurements. Journal of Geophysical Research, 2005, 110, .	3.3	11

#	Article	IF	CITATIONS
397	Collisionless reconnection: mechanism of self-ignition in thin plane homogeneous current sheets. Annales Geophysicae, 2010, 28, 1935-1943.	0.6	11
398	A note on the Weibel instability and thermal fluctuations. Annales Geophysicae, 2012, 30, 427-431.	0.6	11
399	Beyond Gibbs-Boltzmann-Shannon: general entropiesââ,¬â€ŧhe Gibbs-Lorentzian example. Frontiers in Physics, 2014, 2, .	1.0	11
400	Radial distribution of magnetic field in earth magnetotail current sheet. Planetary and Space Science, 2014, 103, 273-285.	0.9	11
401	Measurements of the Vorticity in the Bursty Bulk Flows. Geophysical Research Letters, 2019, 46, 10322-10329.	1.5	11
402	Substorm signatures between 10 and 30 earth radii. Advances in Space Research, 2000, 25, 1663-1666.	1.2	10
403	Evidence for interplanetary magnetic fieldBycontrolled large-scale reconnection at the dayside magnetopause. Journal of Geophysical Research, 2000, 105, 27497-27507.	3.3	10
404	Constraints on magnetic fluctuation energies in the plasma sheet. Geophysical Research Letters, 2001, 28, 919-922.	1.5	10
405	Multi-point study of the magnetotail current sheet. Advances in Space Research, 2006, 38, 85-92.	1.2	10
406	Local fieldâ€aligned currents in the magnetotail and ionosphere as observed by a Cluster, Double Star, and MIRACLE conjunction. Journal of Geophysical Research, 2008, 113, .	3.3	10
407	Magnetic field amplification in electron phase-space holes and related effects. Annales Geophysicae, 2012, 30, 711-724.	0.6	10
408	On the increasing oscillation period of flows at the tailward retreating flux pileup region during dipolarization. Journal of Geophysical Research: Space Physics, 2014, 119, 6603-6611.	0.8	10
409	Anharmonic oscillatory flow braking in the Earth's magnetotail. Geophysical Research Letters, 2015, 42, 3700-3706.	1.5	10
410	Anisotropic Jüttner (relativistic Boltzmann) distribution. Annales Geophysicae, 2016, 34, 737-738.	0.6	10
411	Ion Bernstein waves in the magnetic reconnection region. Annales Geophysicae, 2016, 34, 85-89.	0.6	10
412	Structure, force balance, and topology of Earth's magnetopause. Science, 2017, 356, 960-963.	6.0	10
413	Electron cyclotron maser instability (ECMI) in strong magnetic guide field reconnection. Annales Geophysicae, 2017, 35, 999-1013.	0.6	10
414	On Multiple Hall‣ike Electron Currents and Tripolar Guide Magnetic Field Perturbations During Kelvinâ€Helmholtz Waves. Journal of Geophysical Research: Space Physics, 2018, 123, 1305-1324.	0.8	10

#	Article	IF	CITATIONS
415	Remote Sensing of the Reconnection Electric Field From In Situ Multipoint Observations of the Separatrix Boundary. Geophysical Research Letters, 2018, 45, 3829-3837.	1.5	10
416	Dipolarization Fronts: Tangential Discontinuities? On the Spatial Range of Validity of the MHD Jump Conditions. Journal of Geophysical Research: Space Physics, 2019, 124, 9963-9975.	0.8	10
417	Solar Orbiter's first Venus flyby: MAG observations of structures and waves associated with the induced Venusian magnetosphere. Astronomy and Astrophysics, 0, , .	2.1	10
418	MMS Direct Observations of Kinetic-scale Shock Self-reformation. Astrophysical Journal Letters, 2020, 901, L6.	3.0	10
419	Fluid and particle signatures of dayside reconnection. Annales Geophysicae, 2001, 19, 1045-1063.	0.6	10
420	EDI convection measurements at 5-6 R <sub>E</sub> in the post-midnight region. Annales Geophysicae, 1999, 17, 1503-1512.	0.6	9
421	Bursts of fast magnetotail flux transport. Advances in Space Research, 2002, 30, 2241-2246.	1.2	9
422	Detailed analysis of low-energy electron streaming in the near-Earth neutral line region during a substorm. Advances in Space Research, 2006, 37, 1382-1387.	1.2	9
423	Venusian bow shock as seen by the ASPERAâ€4 ion instrument on Venus Express. Journal of Geophysical Research, 2010, 115, .	3.3	9
424	Relativistic transformation of phase-space distributions. Annales Geophysicae, 2011, 29, 1259-1265.	0.6	9
425	Probabilities of magnetic reconnection encounter at different activity levels in the Earth's magnetotail. Advances in Space Research, 2015, 56, 736-741.	1.2	9
426	Carriers of the Fieldâ€Aligned Currents in the Plasma Sheet Boundary Layer: An MMS Multicase Study. Journal of Geophysical Research: Space Physics, 2019, 124, 2873-2886.	0.8	9
427	Small Spatialâ€5cale Fieldâ€Aligned Currents in the Plasma Sheet Boundary Layer Surveyed by Magnetosphere Multiscale Spacecraft. Journal of Geophysical Research: Space Physics, 2019, 124, 9976-9985.	0.8	9
428	Anisotropic Vorticity Within Bursty Bulk Flow Turbulence. Journal of Geophysical Research: Space Physics, 2020, 125, e2020JA028255.	0.8	9
429	Mission Data Processor Aboard the BepiColombo Mio Spacecraft: Design and Scientific Operation Concept. Space Science Reviews, 2020, 216, 1.	3.7	9
430	Resonant harmonic Alfvén waves in the magnetosphere: A case study. Journal of Geophysical Research, 1984, 89, 10757-10762.	3.3	8
431	Latitude-integrated Joule and particle heating rates during the Energy Budget Campaign. Journal of Atmospheric and Solar-Terrestrial Physics, 1985, 47, 27-39.	0.9	8
432	Observations of correlated broadband electrostatic noise and electron cyclotron emissions in the plasma sheet. Geophysical Research Letters, 1991, 18, 53-56.	1.5	8

#	Article	IF	CITATIONS
433	Local time occurrence frequency of energetic ions in the Earth's magnetosheath. Geophysical Research Letters, 1993, 20, 551-554.	1.5	8
434	Substorm observations in the early morning sector with Equator-S and Geotail. Annales Geophysicae, 1999, 17, 1602-1610.	0.6	8
435	The role of nonlinear interaction in the formation of LF whistler turbulence upstream of a quasi-perpendicular shock. Journal of Geophysical Research, 1999, 104, 12525-12535.	3.3	8
436	Reconstruction of the reconnection rate from Cluster measurements: Method improvements. Journal of Geophysical Research, 2007, 112, .	3.3	8
437	Study of waves in the magnetotail region with cluster and DSP. Advances in Space Research, 2008, 41, 1593-1597.	1.2	8
438	Study of reconnectionâ€associated multiscale fluctuations with Cluster and Double Star. Journal of Geophysical Research, 2008, 113, .	3.3	8
439	Tailward propagation of Pi2 waves in the Earth's magnetotail lobe. Annales Geophysicae, 2008, 26, 4023-4030.	0.6	8
440	Evolution of kinklike fluctuations associated with ion pickup within reconnection outflows in the Earth's magnetotail. Physics of Plasmas, 2009, 16, 120701.	0.7	8
441	Enable the inherent omni-directionality of an absolute coupled dark state magnetometer for e.g. scientific space applications. , 2012, , .		8
442	The strongest magnetic fields in the universe: how strong can they become?. Frontiers in Physics, 2014, 2, .	1.0	8
443	Statistical characteristics of slow earthward and tailward flows in the plasma sheet. Journal of Geophysical Research: Space Physics, 2015, 120, 6199-6206.	0.8	8
444	Hemispheric asymmetry in the nearâ€Venusian magnetotail during solar maximum. Journal of Geophysical Research: Space Physics, 2016, 121, 4542-4547.	0.8	8
445	Accelerated endurance test of single-mode vertical-cavity surface-emitting lasers under vacuum used for a scalar space magnetometer. Applied Physics B: Lasers and Optics, 2018, 124, 1.	1.1	8
446	Electron mirror branch: observational evidence from "historical―AMPTE-IRM and Equator-S measurements. Annales Geophysicae, 2018, 36, 1563-1576.	0.6	8
447	On the applicability of Taylor's hypothesis in streaming magnetohydrodynamic turbulence. Earth, Planets and Space, 2019, 71, .	0.9	8
448	Pickâ€Up Ion Cyclotron Waves Around Mercury. Geophysical Research Letters, 2021, 48, e2021GL092606.	1.5	8
449	The storm time central plasma sheet. Annales Geophysicae, 2002, 20, 1737-1741.	0.6	8
450	Thin Current Sheet Behind the Dipolarization Front. Journal of Geophysical Research: Space Physics, 2021, 126, e2021JA029518.	0.8	8

#	Article	IF	CITATIONS
451	First ELF wave measurements with the Equator-S magnetometer. Advances in Space Research, 1999, 24, 77-80.	1.2	7
452	Substorm expansion onset mechanism debated. Eos, 2000, 81, 70.	0.1	7
453	Equatorial, Birkeland, and Ionospheric Currents of the Magnetospheric Storm Circuit. Geophysical Monograph Series, 0, , 111-122.	0.1	7
454	Heating and Fast Flows in the Near-Earth Tail. Geophysical Monograph Series, 0, , 141-145.	0.1	7
455	Evidence of transient reconnection in the outflow jet of primary reconnection site. Annales Geophysicae, 2014, 32, 239-248.	0.6	7
456	A statistical study of the lowâ€eltitude ionospheric magnetic fields over the north pole of Venus. Journal of Geophysical Research: Space Physics, 2015, 120, 6218-6229.	0.8	7
457	Dayside Convection, Viscous Interaction and Magnetic Merging. Astrophysics and Space Science Library, 1986, , 415-421.	1.0	7
458	Magnetometer in-flight offset accuracy for the BepiColombo spacecraft. Annales Geophysicae, 2020, 38, 823-832.	0.6	7
459	Suprathermal ion fluxes in the plasma sheet. Geophysical Research Letters, 1990, 17, 275-278.	1.5	6
460	Near-Earth plasma sheet dynamics. Advances in Space Research, 1996, 18, 27-33.	1.2	6
461	EDI electron time-of-flight measurements on Equator-S. Annales Geophysicae, 1999, 17, 1513-1520.	0.6	6
462	Dynamics and local boundary properties of the dawn-side magnetopause under conditions observed by Equator-S. Annales Geophysicae, 1999, 17, 1535-1559.	0.6	6
463	Collisionless mirror mode trapping. Nonlinear Processes in Geophysics, 2000, 7, 179-184.	0.6	6
464	Compressional Pc5 pulsations as sloshing in the plasma sheet. Journal of Geophysical Research, 2000, 105, 23287-23292.	3.3	6
465	Equator-S observations of ion cyclotron waves outside the dawnside magnetopause. Journal of Geophysical Research, 2002, 107, SMP 4-1.	3.3	6
466	MHD-modelling of the magnetosheath. Planetary and Space Science, 2002, 50, 473-488.	0.9	6
467	Magnetospheric Contributions to the Terrestrial Magnetic Field. , 2007, , 77-92.		6
468	Simultaneous FAST and Double Star TC1 observations of broadband electrons during a storm time substorm. Journal of Geophysical Research, 2010, 115, .	3.3	6

#	Article	IF	CITATIONS
469	Magnetopause displacements: the possible role of dust. Annales Geophysicae, 2011, 29, 2219-2223.	0.6	6
470	Ion and Electron Heating in the Near-Earth Tail. Geophysical Monograph Series, 0, , 97-102.	0.1	6
471	Plasma wave mediated attractive potentials: a prerequisite for electron compound formation. Annales Geophysicae, 2014, 32, 975-989.	0.6	6
472	Parallelâ€dominant and perpendicularâ€dominant components of the fast bulk flow: Comparing with the PSBL beams. Journal of Geophysical Research: Space Physics, 2015, 120, 9500-9512.	0.8	6
473	Occurrence rate of dipolarization fronts in the plasma sheet: Cluster observations. Annales Geophysicae, 2017, 35, 1015-1022.	0.6	6
474	On the ion-inertial-range density-power spectra in solar wind turbulence. Annales Geophysicae, 2019, 37, 183-199.	0.6	6
475	Statistical Characteristics of Fieldâ€Aligned Currents in the Plasma Sheet Boundary Layer. Journal of Geophysical Research: Space Physics, 2021, 126, e2020JA028319.	0.8	6
476	Braking of High-Speed Flow and Azimuthal Pressure Gradient as Driving Forces of Substorm Currents. Astrophysics and Space Science Library, 1998, , 355-360.	1.0	6
477	Electric fields derived from electron drift measurements. Geophysical Research Letters, 1994, 21, 1863-1866.	1.5	5
478	Recent advances, open questions and future directions in solar-terrestrial research. Physics and Chemistry of the Earth, Part C: Solar, Terrestrial and Planetary Science, 1999, 24, 5-28.	0.2	5
479	The magnetopause at high time resolution: Structure and lower-hybrid waves. Geophysical Research Letters, 2001, 28, 681-684.	1.5	5
480	Climate and weather of the Sun–Earth system: CAWSES. Advances in Space Research, 2004, 34, 443-448.	1.2	5
481	What is Cluster telling us about magnetotail dynamics?. Advances in Space Research, 2005, 36, 1909-1915.	1.2	5
482	Magnetospheric Contributions to the Terrestrial Magnetic Field. , 2007, , 79-90.		5
483	Cluster observations of broadband ULF waves near the dayside polar cap boundary: Two detailed multiâ€instrument event studies. Journal of Geophysical Research, 2007, 112, .	3.3	5
484	Conjugate observation of sharp dynamical boundary in the inner magnetosphere by Cluster and DMSP spacecraft and ground network. Annales Geophysicae, 2008, 26, 2771-2780.	0.6	5
485	Corrigendum to "Substorm activity in Venus's magnetotail" published in Ann. Geophys., 27, 2321–2330, doi:10.5194/angeo-27-2321-2009, 2009. Annales Geophysicae, 2010, 28, 1877-1878.	0.6	5

486 Control loops for a Coupled Dark State Magnetometer. , 2010, , .

#	Article	IF	CITATIONS
487	Remote estimation of reconnection parameters in the Earth's magnetotail: model and observations. Annales Geophysicae, 2012, 30, 1727-1741.	0.6	5
488	Superdiffusion revisited in view of collisionless reconnection. Annales Geophysicae, 2014, 32, 643-650.	0.6	5
489	The differential cosmic ray energy flux in the light of an ultrarelativistic generalized Lorentzian thermodynamics. Astrophysics and Space Science, 2018, 363, 1.	0.5	5
490	The mirror mode: a "superconducting―space plasma analogue. Annales Geophysicae, 2018, 36, 1015-1026.	0.6	5
491	A Note on the Entropy Force in Kinetic Theory and Black Holes. Entropy, 2019, 21, 716.	1.1	5
492	Continentâ€Wide R1/R2 Current System and Ohmic Losses by Broad Dipolarizationâ€Injection Fronts. Journal of Geophysical Research: Space Physics, 2019, 124, 4064-4082.	0.8	5
493	MMS Observations of Reconnection Separatrix Region in the Magnetotail at Different Distances From the Active Neutral Xâ€Line. Journal of Geophysical Research: Space Physics, 2021, 126, e2020JA028694.	0.8	5
494	Brief Communication: Weibel, Firehose and Mirror mode relations. Nonlinear Processes in Geophysics, 2014, 21, 143-148.	0.6	5
495	The Electron Drift Instrument for Cluster. , 1997, , 233-269.		5
496	The AMPTE lithium releases in the solar wind: A possible trigger for geomagnetic pulsations. Geophysical Research Letters, 1990, 17, 2301-2304.	1.5	4
497	Ion signatures of reconnection at the magnetopause. Advances in Space Research, 1997, 19, 1947-1950.	1.2	4
498	Dawnside magnetopause observed by the Equator-S Magnetic Field Experiment: Identification and survey of crossings. Journal of Geophysical Research, 1999, 104, 17491-17497.	3.3	4
499	Observation of reconnection pulses by Cluster and Double Star. Annales Geophysicae, 2005, 23, 2921-2927.	0.6	4
500	Structure of the near-Earth plasma sheet during tailward flows. Annales Geophysicae, 2008, 26, 709-724.	0.6	4
501	THEMIS observations of consecutive bursts of Pi2 pulsations: The 20 April 2007 event. Journal of Geophysical Research, 2009, 114, .	3.3	4
502	ls current disruption associated with an inverse cascade?. Nonlinear Processes in Geophysics, 2010, 17, 287-292.	0.6	4
503	THEMIS observations of double-onset substorms and their association with IMF variations. Annales Geophysicae, 2011, 29, 591-611.	0.6	4
504	On the evolution of a magnetic flux rope: Twoâ€dimensional MHD simulation results. Journal of Geophysical Research: Space Physics, 2015, 120, 8547-8558.	0.8	4

#	Article	IF	CITATIONS
505	Ideal MHD turbulence: the inertial range spectrum with collisionless dissipation. Frontiers in Physics, 2015, 3, .	1.0	4
506	Earthward and tailward flows in the plasma sheet. Journal of Geophysical Research: Space Physics, 2015, 120, 4487-4495.	0.8	4
507	Temporal evolutions of the solar wind conditions at 1 AU prior to the nearâ€Earth X lines in the tail: Superposed epoch analysis. Journal of Geophysical Research: Space Physics, 2016, 121, 7488-7496.	0.8	4
508	Scaling laws in Hall inertial-range turbulence. Annales Geophysicae, 2019, 37, 825-834.	0.6	4
509	MMS Observation on the Crossâ€Tail Current Sheet Rollâ€up at the Dipolarization Front. Journal of Geophysical Research: Space Physics, 2021, 126, e2020JA028796.	0.8	4
510	Magnetosheath plasma flow model around Mercury. Annales Geophysicae, 2021, 39, 563-570.	0.6	4
511	First Results of the THEMIS Search Coil Magnetometers. , 2009, , 509-534.		4
512	Vorticity Within Bursty Bulk Flows: Convective Versus Kinetic. Journal of Geophysical Research: Space Physics, 2022, 127, .	0.8	4
513	Trapping conditions for energetic particles incident on a tangential discontinuity surface. Planetary and Space Science, 1987, 35, 483-485.	0.9	3
514	Substorms and flux rope structures. Geophysical Monograph Series, 1990, , 627-635.	0.1	3
515	Proton pitch angle diffusion rate and wave turbulence characteristics in the magnetosheath plasma. Journal of Geophysical Research, 2002, 107, SMP 35-1.	3.3	3
516	A new processing method for the AE index. Science in China Series D: Earth Sciences, 2008, 51, 1713-1720.	0.9	3
517	Plasma sheet oscillations and their relation to substorm development: Cluster and double star TC1 case study. Advances in Space Research, 2008, 41, 1585-1592.	1.2	3
518	Publisher's Note: New Features of Electron Phase Space Holes Observed by the THEMIS Mission [Phys. Rev. Lett. <b>102</b> , 225004 (2009)]. Physical Review Letters, 2009, 103, .	2.9	3
519	Flux quanta, magnetic field lines, merging – some sub-microscale relations of interest in space plasma physics. Annales Geophysicae, 2011, 29, 1121-1127.	0.6	3
520	Association of consecutive Pi2â€₽s6 band pulsations with earthward fast flows in the plasma sheet in response to IMF variations. Journal of Geophysical Research: Space Physics, 2014, 119, 3617-3640.	0.8	3
521	Auroral Kilometric Radiation and Electron Pairing. Frontiers in Physics, 2020, 8, .	1.0	3
522	Lorentzian Entropies and Olbert's κ - Distribution. Frontiers in Physics, 2020, 8, .	1.0	3

#	Article	IF	CITATIONS
523	Venus's induced magnetosphere during active solar wind conditions at BepiColombo's Venus 1 flyby. Annales Geophysicae, 2021, 39, 811-831.	0.6	3
524	Hermean Magnetosphere-Solar Wind Interaction. Space Sciences Series of ISSI, 2008, , 347-368.	0.0	3
525	The FIELDS Instrument Suite on MMS: Scientific Objectives, Measurements, and Data Products. , 2017, , 105-135.		3
526	The interaction of impulsive solar wind discontinuities with the magnetosphere: A multi-satellite case study. Planetary and Space Science, 1990, 38, 841-850.	0.9	2
527	The decay of suprathermal ion fluxes during the substorm recovery phase. Journal of Geophysical Research, 1994, 99, 10941.	3.3	2
528	Reply [to "Comment on "Current understanding of magnetic storms: Storm-substorm relationships,― by Y. Kamide et al.â€]. Journal of Geophysical Research, 1999, 104, 7051-7051.	3.3	2
529	Equator-S magnetopause crossings at high time resolution. Journal of Geophysical Research, 2001, 106, 25409-25418.	3.3	2
530	Substorms, storms, and the storm-time plasma sheet. Geophysical Monograph Series, 2003, , 55-58.	0.1	2
531	Correction to "GEOTAIL encounter with magnetic reconnection diffusion region in the Earth's magnetotail: Evidence of multiple x-lines collisionless reconnectionâ€. Journal of Geophysical Research, 2004, 109, .	3.3	2
532	Structures of magnetic null points in reconnection diffusion region: Cluster observations. Science Bulletin, 2008, 53, 1880-1886.	4.3	2
533	Convective high-speed flow and field-aligned high-speed flows explored by TC-1. Science Bulletin, 2008, 53, 2371-2375.	4.3	2
534	Oscillation of electron counts at 500 eV downstream of the quasiâ€perpendicular bow shock. Journal of Geophysical Research, 2008, 113, .	3.3	2
535	Estimating the magnetic energy inside traveling compression regions. Annales Geophysicae, 2009, 27, 1969-1978.	0.6	2
536	Collisionless reconnection: magnetic field line interaction. Annales Geophysicae, 2012, 30, 1515-1528.	0.6	2
537	AMPTE-IRM Observations of Particles and Fields at the Dayside Low-latitude Magnetopause. Geophysical Monograph Series, 2013, , 51-65.	0.1	2
538	Broad current sheets, current bifurcation, and collisionless reconnectionââ,¬â€An Opinion on ââ,¬Å"Onset of fast magnetic reconnection via subcritical bifurcationââ,¬Â•by Z. Guo and X. Wang. Frontiers in Physics, 2015, 3, .	1.0	2
539	Possible increased critical temperature Tc in anisotropic bosonic gases. Scientific Reports, 2019, 9, 10339.	1.6	2
540	Electron pairing in mirror modes: surpassing the quasi-linear limit. Annales Geophysicae, 2019, 37, 971-988.	0.6	2

#	Article	IF	CITATIONS
541	Mirror Mode Junctions as Sources of Radiation. Frontiers in Astronomy and Space Sciences, 2021, 8, .	1.1	2
542	The usefulness of Poynting's theorem in magnetic turbulence. Annales Geophysicae, 2017, 35, 1353-1360.	0.6	2
543	Current Systems in Planetary Magnetospheres and Ionospheres. Space Sciences Series of ISSI, 2010, , 99-134.	0.0	2
544	Fundamental effective temperature measurements for eclipsing binary stars – III. SPIRou near-infrared spectroscopy and CHEOPS photometry of the benchmark GOV star EBLMÂJ0113+31. Monthly Notices of the Royal Astronomical Society, 0, , .	1.6	2
545	Examples of multi-instrumental studies on auroral phenomena. , 1982, , 124-133.		1
546	Magnetometer networks in northern Europe. , 1982, , 134-140.		1
547	Dayside High-Latitude Ionospheric Current Systems. , 1985, , 223-234.		1
548	AMPTE/IRM observations of the MHD Structure of the plasmasheet boundary: Evidence for a normal component of the magnetic field. Geophysical Monograph Series, 1995, , 357-363.	0.1	1
549	Magnetopause boundary structure deduced from the high-time resolution particle experiment on the Equator-S spacecraft. Annales Geophysicae, 1999, 17, 1574-1581.	0.6	1
550	Plasma Sheet Expansion Observed by Cluster and Geotail. COSPAR Colloquia Series, 2005, , 177-185.	0.2	1
551	Unexpected vertical current sheets in the magnetotail associated with northward IMF. Advances in Space Research, 2005, 36, 1830-1834.	1.2	1
552	Near-Earth bursty bulk flows and AE index. Science in China Series D: Earth Sciences, 2008, 51, 1704-1712.	0.9	1
553	Multipoint observations of plasma distributions around an X line. , 2009, , .		1
554	Downward auroral currents from the reconnection Hall-region. Annales Geophysicae, 2011, 29, 679-685.	0.6	1
555	The transterminator ion flow at Venus at solar minimum. Planetary and Space Science, 2012, 73, 341-346.	0.9	1
556	Magnetic field topology of the plasma sheet boundary layer. Journal of Geophysical Research: Space Physics, 2013, 118, 4059-4065.	0.8	1
557	Incomplete-exclusion statistical mechanics in violent relaxation. Astronomy and Astrophysics, 2013, 558, A40.	2.1	1
558	Fractional Laplace transformsââ,¬â€a perspective. Frontiers in Physics, 2014, 2, .	1.0	1

#	Article	IF	CITATIONS
559	Generalised partition functions: inferences on phase space distributions. Annales Geophysicae, 2016, 34, 557-564.	0.6	1
560	Inverse scattering problem in turbulent magnetic fluctuations. Annales Geophysicae, 2016, 34, 673-689.	0.6	1
561	Critical temperature in relativistic Lorentzian thermodynamics of massive bosons. Europhysics Letters, 2016, 116, 10003.	0.7	1
562	Causal kinetic equation of non-equilibrium plasmas. Annales Geophysicae, 2017, 35, 683-690.	0.6	1
563	Substormâ€Related Nearâ€Earth Reconnection Surge: Combining Telescopic and Microscopic Views. Geophysical Research Letters, 2019, 46, 6239-6247.	1.5	1
564	Olbertian Partition Function in Scalar Field Theory. Frontiers in Physics, 2020, 8, .	1.0	1
565	Olbert's Kappa Fermi and Bose Distributions. Frontiers in Physics, 2021, 9, .	1.0	1
566	Results of the Electron Drift Instrument on Cluster. Journal of Geophysical Research: Space Physics, 2021, 126, e2021JA029313.	0.8	1
567	Expansion Phase Signatures in the Tail between 11 and 31 Earth Radii. Astrophysics and Space Science Library, 1998, , 203-206.	1.0	1
568	The Magnetospheric Multiscale Magnetometers. , 2016, 199, 189.		1
569	SCALE-DEPENDENT ANISOTROPY OF MAGNETIC FLUCTUATIONS IN THE EARTH'S PLASMA SHEET. , 2005, , 29-38.		1
570	NONEXTENSIVE ENTROPY APPROACH TO SPACE PLASMA FLUCTUATIONS AND TURBULENCE. , 0, , 43-64.		1
571	EDI convection measurements at 5–6 R. Annales Geophysicae, 1999, 17, 1503.	0.6	1
572	Detection of the tidal deformation of WASP-103b at 3 <i>Ïf </i> with CHEOPS <i>(Corrigendum)</i> . Astronomy and Astrophysics, 2022, 658, C1.	2.1	1
573	The AMPTE IRM Science Data Center. IEEE Transactions on Geoscience and Remote Sensing, 1985, GE-23, 216-220.	2.7	0
574	Erdmagnetismus und extraterrestrische Vorg�nge. Die Naturwissenschaften, 1987, 74, 181-187.	0.6	0
575	Reply [to "Comment on †Braking of high-speed flows in the near-Earth Tail' by K. Shiokawa, W. Baumjohann, and G. Haerendelâ€]. Geophysical Research Letters, 1998, 25, 3503-3503.	1.5	0

576 Some signatures of magnetic field line reconnection. , 2002, , .

#	Article	IF	CITATIONS
577	Scales in a thinning plasma sheet. , 2009, , .		0
578	The Cross-Scale Mission. , 2009, , .		0
579	Radial propagation velocity of energetic particle injections according to measurements onboard the Cluster satellites. Cosmic Research, 2009, 47, 22-28.	0.2	Ο
580	Correction to "Intermittent turbulence, noisy fluctuations, and wavy structures in the Venusian magnetosheath and wake― Journal of Geophysical Research, 2009, 114, .	3.3	0
581	Corrigendum to "Downward auroral currents from the reconnection Hall-region", published in Ann. Geophys., 29, 679–685, 2011. Annales Geophysicae, 2011, 29, 1061-1061.	0.6	Ο
582	Magnetic susceptibility from electron holes. Annales Geophysicae, 2013, 31, 1191-1193.	0.6	0
583	Lessons on collisionless reconnection from quantum fluids. Frontiers in Physics, 2014, 2, .	1.0	0
584	Kinetic theory of informationââ,¬â€ŧhe dynamics of information. Frontiers in Physics, 2015, 3, .	1.0	0
585	Information kineticsââ,¬â€an extension. Frontiers in Physics, 2015, 3, .	1.0	Ο
586	Topside Reconnection. Frontiers in Physics, 2020, 8, .	1.0	0
587	Condensate Formation in Collisionless Plasma. Frontiers in Physics, 2021, 9, .	1.0	0
588	Diffuse Josephson Radiation in Turbulence. Frontiers in Physics, 2021, 9, .	1.0	0
589	<i>Erratum</i> Fluid and particle signatures of dayside reconnection. Annales Geophysicae, 2002, 20, 583-583.	0.6	0
590	Particle Acceleration in Mercury's Magnetosphere. Space Sciences Series of ISSI, 2008, , 411-427.	0.0	0
591	Equator-S: Mission and First Results. , 1999, , 1-10.		0
592	The Electron Drift Instrument for MMS. , 2017, , 283-305.		0
593	Long-term vacuum tests of single-mode vertical cavity surface emitting laser diodes used for a scalar magnetometer. , 2017, , .		0